

Determination of Hydrogen Bond Structure in Water versus Aprotic Environments To Test the Relationship Between Length and Stability

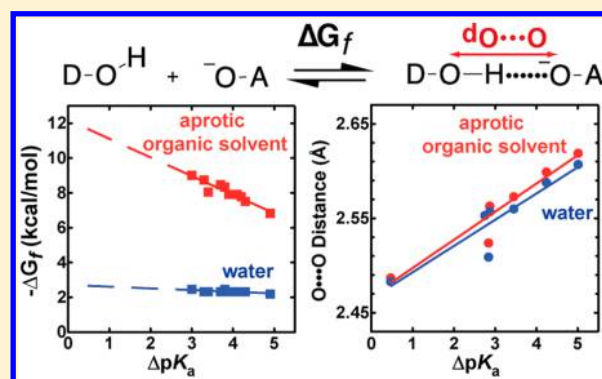
Paul A. Sigala,^{†,∇} Eliza A. Ruben,[†] Corey W. Liu,[‡] Paula M. B. Piccoli,[§] Edward G. Hohenstein,[#] Todd J. Martínez,[#] Arthur J. Schultz,^{§,||} and Daniel Herschlag^{*,†,#}

[†]Department of Biochemistry, [‡]Stanford Magnetic Resonance Laboratory, and [#]Department of Chemistry, Stanford University, Stanford, California 94305, United States

[§]Intense Pulsed Neutron Source, Argonne National Laboratory, Argonne, Illinois 60439, United States

S Supporting Information

ABSTRACT: Hydrogen bonds profoundly influence the architecture and activity of biological macromolecules. Deep appreciation of hydrogen bond contributions to biomolecular function thus requires a detailed understanding of hydrogen bond structure and energetics and the relationship between these properties. Hydrogen bond formation energies (ΔG_f) are enormously more favorable in aprotic solvents than in water, and two classes of contributing factors have been proposed to explain this energetic difference, focusing respectively on the isolated and hydrogen-bonded species: (I) water stabilizes the dissociated donor and acceptor groups much better than aprotic solvents, thereby reducing the driving force for hydrogen bond formation; and (II) water lengthens hydrogen bonds compared to aprotic environments, thereby decreasing the potential energy within the hydrogen bond. Each model has been proposed to provide a dominant contribution to ΔG_f , but incisive tests that distinguish the importance of these contributions are lacking. Here we directly test the structural basis of model II. Neutron crystallography, NMR spectroscopy, and quantum mechanical calculations demonstrate that O–H···O hydrogen bonds in crystals, chloroform, acetone, and water have nearly identical lengths and very similar potential energy surfaces despite ΔG_f differences >8 kcal/mol across these solvents. These results rule out a substantial contribution from solvent-dependent differences in hydrogen bond structure and potential energy after association (model II) and thus support the conclusion that differences in hydrogen bond ΔG_f are predominantly determined by solvent interactions with the dissociated groups (model I). These findings advance our understanding of universal hydrogen-bonding interactions and have important implications for biology and engineering.



INTRODUCTION

Hydrogen bonds are ubiquitous chemical interactions whose formation and properties contribute enormously to protein and nucleic acid folding, molecular recognition, enzymatic catalysis, and drug–receptor interactions. A thorough understanding of hydrogen bond structure and energetics is thus required to deeply understand hydrogen bond contributions to biomolecular function and to optimize the engineering of new molecular systems with novel functional properties. In this work, we test the relationship between hydrogen bond length and the free energy change (ΔG_f) upon hydrogen bond formation. ΔG_f reflects the overall stability of a hydrogen-bonded complex relative to the dissociated donor and acceptor groups (Figure 1A) and is the most common thermodynamic measure for assessing hydrogen bond contributions to protein folding, ligand binding, and enzyme catalysis.¹

Substantial prior work has indicated that the energetic properties of hydrogen bonds are strongly influenced by the nature of the surrounding environment. Extensive studies of small-molecule complexes have provided overwhelming

evidence that hydrogen bonds formed in aprotic environments are enormously more stable than in water. For example, ΔG_f for hydrogen bond formation between 4-nitrophenol and 4-nitrophenolate is 7–8 kcal/mol more favorable in acetonitrile and tetrahydrofuran than in water, and the hydrogen bond between fluoride and hydrogen fluoride is nearly 40 kcal/mol more stable in the gas phase than in water.^{2–5}

Particular attention has been focused in the literature on the structural and energetic role of hydrogen bonds with lengths of 2.4–2.6 Å, as these hydrogen bonds are significantly shorter than the majority of 2.8–3.2 Å hydrogen bonds observed in protein and small-molecule structures. Such short hydrogen bonds display distinguishing spectroscopic features (e.g., ¹H NMR chemical shifts of 14–18 ppm) in aprotic organic solvents, have large formation free energies in aprotic environments, and are frequently referred to as “short, strong hydrogen bonds”.^{6–10} In contrast, spectroscopic signals

Received: December 21, 2014

Published: April 14, 2015

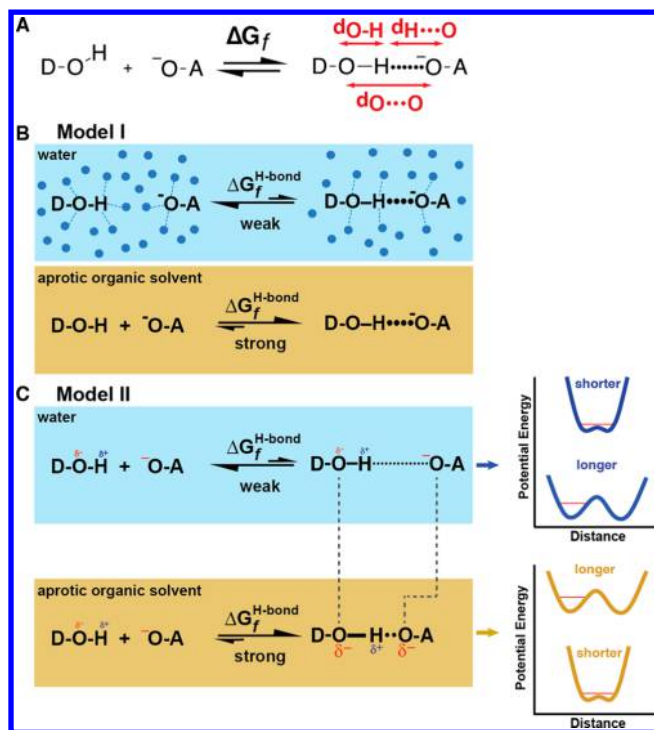


Figure 1. Models for the effect of solvent on the equilibrium formation of O–H⋯O[−] hydrogen bonds. (A) Schematic depiction of hydrogen bond lengths and formation free energy (ΔG_f), which reflects the stability of the hydrogen-bonded complex relative to the dissociated groups. (B) Schematic depiction of model I in which hydrogen bond stability is determined by the differential interactions of water versus aprotic solvents with the dissociated donor and acceptor groups, with identical hydrogen-bonded species in the differing solvents. (C) Schematic depiction of model II in which solvent–solute interactions lengthen a hydrogen bond in water relative to an aprotic organic solvent, resulting in the longer hydrogen bond as the more stable structure in water and the shorter hydrogen bond as the more stable structure in an aprotic environment. Charges and partial charges depict possible effects that accompany hydrogen bond shortening and interactions with solvent molecules. The larger dots represent the deeper potential energy well posited in aprotic organic solvents according to model II.

indicative of short hydrogen bonds have not typically been observed for hydrogen-bonded complexes in water,^{8,11} where ΔG_f values are small.

Based on these structural and energetic observations, two general models have been proposed in the literature to account for the enhanced stabilities of hydrogen bonds in aprotic environments compared to water. These models can provide independent and additive contributions to ΔG_f and focus on either the dissociated donor and acceptor groups (Figure 1A, left side of equilibrium) or the hydrogen-bonded complex (Figure 1A, right side of equilibrium) and the differential effects of the surroundings on these species, as elaborated below (see additional discussion in Text S1, Supporting Information).

Model I addresses the differential ability of protic versus aprotic solvents to stabilize the separated hydrogen bond donor and acceptor groups.^{2,3,12–14} According to proposals that this model provides a dominant contribution to hydrogen bond ΔG_f , the isolated charge of a dissociated oxyanionic acceptor will be enormously more stable in water than in aprotic organic solvents, resulting in a substantially reduced hydrogen bond

formation energy in water compared to aprotic environments (Figure 1B).

Model II addresses the hydrogen-bonded complex and posits that hydrogen bonds adopt shorter equilibrium distances in aprotic environments than in water and that such shortening deepens the potential energy well of the hydrogen-bonded groups and results in a much more favorable formation free energy (Figure 1C, additional discussion in Text S1).^{8,12,15–23}

This model recognizes that hydrogen bonds are largely electrostatic in character but have a charge-transfer component that increases as a hydrogen bond shortens due to enhanced orbital overlap.^{24,25} Hydrogen bonds formed in water might be preferentially longer due to favorable interactions between more localized charges and solvent water molecules (Figure 1C). In the absence of strong stabilizing interactions with solvent, hydrogen bonds formed in aprotic solvents might instead adopt shorter distances to maximize stabilization from charge delocalization (see additional discussion in Text S1 and S2). Indeed, a prior computational study suggested that the O⋯O distance of the water–hydroxide hydrogen bond lengthens from 2.4 Å in the gas phase to 2.8 Å in water.¹²

Both models have been suggested to be important for protein function. For example, “short, strong hydrogen bonds” have been proposed to form within buried protein interiors, due to unique properties of the solvent-sequestered protein matrix that differ from water, and to contribute substantially to enzyme catalysis because of their short lengths.^{6,9,11,19} Other researchers have invoked the general observation of increased hydrogen bond formation free energies in the absence of water to suggest that hydrogen bond stability might be enhanced within protein interiors due to loop or domain closures or the tight packing of active site groups that largely exclude bulk water molecules.^{26,27}

Despite the ubiquity of the two models described above, the relative importance of their energetic contributions to hydrogen bond stability in solution has never been distinguished and assessed. Indeed, the central tenet of the second model that hydrogen bonds are longer in water than in nonaqueous environments has remained untested due to technical challenges in assessing hydrogen bond structure in water. There have been occasional spectroscopic reports^{9,28–31} suggesting that short hydrogen bond distances can form in partially aqueous environments at subzero temperatures (e.g., 10% water/90% acetone at -50 °C), and X-ray crystallographic studies of the 4-nitrophenol–4-nitrophenolate complex have reported nearly identical O⋯O distances in the absence (2.475 Å) or presence (2.465 Å) of two hydrating water molecules per unit cell.³² Under these heterogeneous and low-temperature conditions, however, the solvation properties of water molecules can substantially differ from bulk water.³³

We have critically assessed the structural basis for model II (Figure 1C) by systematically testing whether hydrogen bonds are longer and have significantly different potential energy surfaces in water relative to aprotic organic solvents. Our results provide direct evidence that the weaker formation free energies observed for hydrogen bonds in water compared to aprotic organic solvents are not accompanied by increased hydrogen bond lengths or substantially differing potential energy surfaces across these environments. These results rule out the central underpinning of model II and, by elimination, support model I as the dominant determinant of hydrogen bond ΔG_f . This finding has important implications for understanding the contributions of hydrogen bonds to the fundamental energetic

and structural properties of biomolecules, their complexes, and their functions.

RESULTS AND DISCUSSION

We approached this question by studying changes across a series of compounds in multiple environments, rather than examining a single hydrogen-bonded complex, as we reasoned that systematic studies could provide more extensive and incisive information about the relationship between solvation and hydrogen bond structure and potential energy surface. We focused on O–H···O hydrogen bonds, as these interactions are common in nature and have been the subject of extensive prior investigation.^{8,25,34,35}

The Dependence of Hydrogen Bond Length on ΔpK_a . Hydrogen bond formation energies (ΔG_f) are commonly observed to depend linearly on ΔpK_a , the proton affinity difference between the hydrogen bond donor and acceptor groups, with the largest formation energies typically observed at or near a ΔpK_a value of zero.^{5,36} As the shortest hydrogen bond lengths are also typically observed between groups with similar pK_a values,³⁷ we first asked whether hydrogen bond lengths also show a broad linear dependence on ΔpK_a . We analyzed the crystal structures in Steiner and Saenger's 1994 compilation of O–H···O hydrogen bonds determined by low-temperature (<130 K) neutron diffraction,³⁵ experimental conditions that most accurately determine proton positions. We also determined low-temperature neutron structures of six additional hydrogen-bonded complexes, resulting in a composite, structurally diverse data set of 68 inter- and intramolecular hydrogen bonds with ΔpK_a values spanning nearly 20 units (Table S1).

We compiled the O···O, O–H, and H···O distances observed in the neutron structures for each hydrogen-bonded complex and plotted these distances as a function of the ΔpK_a values determined for each hydrogen bond based on the experimental or calculated pK_a values of the interacting donor and acceptor groups. These plots revealed a steady dependence on ΔpK_a , with the O···O distance increasing linearly with a slope of 0.02 Å/ pK_a unit from 2.4 Å to almost 2.9 Å as ΔpK_a increased from 0 to 20 ($R^2 = 0.86$) (Figure 2A). The position of the hydrogen-bonded proton also varied steadily with ΔpK_a , with both O–H and H···O distances converging on 1.2 Å as ΔpK_a approached zero (Figure 2B).

This structural dependence on ΔpK_a observed directly by neutron diffraction is consistent with prior NMR and IR studies of O–H···O hydrogen bonds in aprotic organic solvents and in the gas phase that have reported systematic changes as a function of ΔpK_a in ^1H chemical shift and O–H stretching frequency, spectroscopic observables that provide incisive readouts of hydrogen bond structure.^{38–41} Our direct assessment of this structural dependence on ΔpK_a in hydrogen-bonded crystals provides a quantitative baseline from which to test and compare the effects of differing solvent environments.

Direct Tests of Hydrogen Bond Structure in Aprotic Solvents versus Water via ^1H NMR. In a nonaqueous environment, both hydrogen bond length and formation free energy correlate with ΔpK_a . Prior studies^{3,36,42} have provided clear evidence that hydrogen bond formation energies display a substantially steeper dependence on ΔpK_a in aprotic organic solvents than in water. The critical unresolved question that we set out to test was whether hydrogen bond lengths also display a steeper dependence on ΔpK_a in aprotic organic solvents than in aqueous solution, as predicted based on the central tenet of

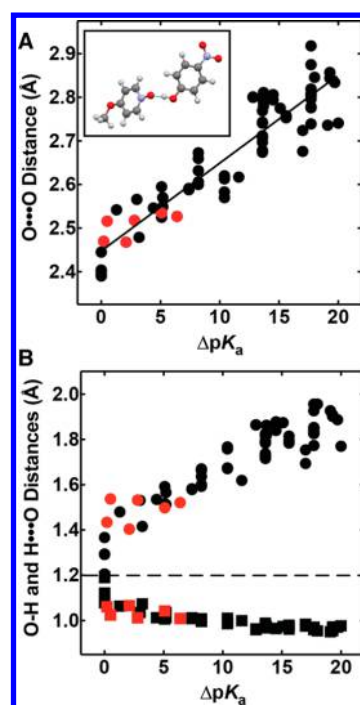


Figure 2. The dependence of hydrogen bond length on ΔpK_a . Dependence of O···O distance ($R^2 = 0.86$) (A) and O–H (squares) and H···O distances (circles) (B) on ΔpK_a for O–H···O hydrogen bonds in low-temperature neutron structures. Data points for newly determined structures are in red. Inset in (A) is the neutron structure for 4-nitrophenol-4-methoxypyridine-*N*-oxide determined herein ($\Delta pK_a = 5.1$). Aqueous pK_a values are used herein as a proxy for proton affinity and so that each compound can be denoted by a single ΔpK_a value that allows comparisons between properties of the same compound in different environments.

model II (Figure 1C) that hydrogen bond formation energies depend directly on hydrogen bond lengths.

We exploited the ability of ^1H NMR spectroscopy to directly detect hydrogen-bonded protons and its high sensitivity to changes in hydrogen bond structure as small as 0.01 Å.³⁴ ^1H chemical shifts from solid-state NMR correlate strongly with hydrogen bond distances determined by neutron diffraction, with the chemical shift of the hydrogen-bonded proton increasing from 12–20 ppm as the O···O distance decreases from 2.7 to 2.4 Å and the O···H distance simultaneously decreases from 1.7 to 1.2 Å.^{23,34,43–46} This correlation has been ascribed to decreased shielding from σ bond electron density around the proton as it migrates away from its covalently associated oxygen toward the center of the hydrogen bond as O···O distances shorten,^{23,35,47} and it provides a powerful means to detect and quantify changes in hydrogen bond structure within solution environments.^{44,48} This approach has been used to interrogate hydrogen bond structure in aprotic solvents,^{8,45,48} but aqueous environments remain challenging to study due to proton exchange between water molecules and hydrogen-bonded solutes.

We focused on the intramolecular hydrogen bond within salicylate monoanions (Figure 3A), as a prior ^1H NMR study²⁹ of these compounds in 10% water/acetone (–50 °C) hinted that it might be possible to detect the hydrogen-bonded proton on a high-field instrument in fully aqueous solution (i.e., 100% water) and thus enable the critical experimental test. Furthermore, these compounds are available with differing

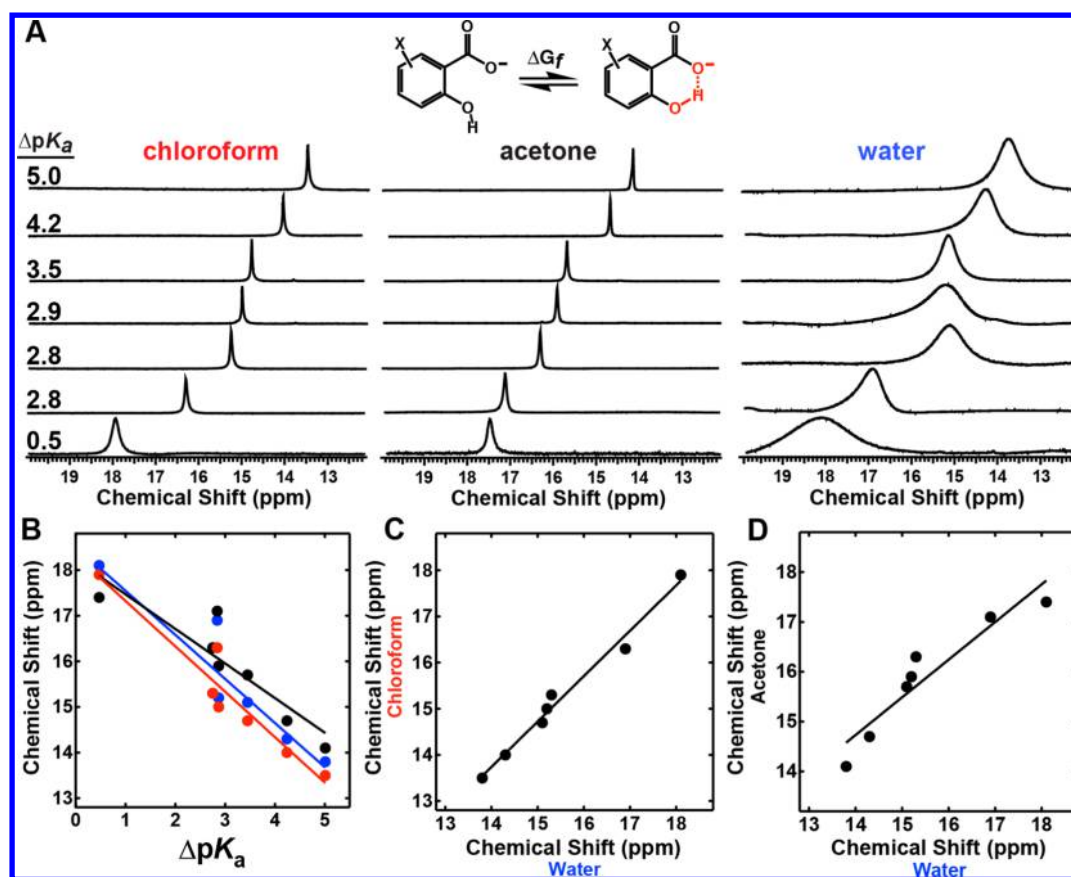


Figure 3. Solution ^1H NMR studies of hydrogen bonding in substituted salicylate monoanions. (A) Schematic depiction of intramolecular hydrogen bond formation in salicylates and ^1H NMR spectra of 5-methylsalicylate ($\Delta pK_a = 5.0$), 4-methoxysalicylate ($\Delta pK_a = 4.2$), 3,5-dichlorosalicylate ($\Delta pK_a = 3.5$), 5-formylsalicylate ($\Delta pK_a = 2.9$), 5-nitrosalicylate ($\Delta pK_a = 2.8$), 3-nitrosalicylate ($\Delta pK_a = 2.8$), and 3,5-dinitrosalicylate ($\Delta pK_a = 0.5$) in chloroform, acetone, and water at 4°C . The spectrum of 3,5-dinitrosalicylate in water was acquired in 90% water/10% DMSO at -3°C . (B–D) Dependence of ^1H NMR chemical shift in each solvent on ΔpK_a (slopes = $0.8\text{--}1.0$ ppm/ pK_a unit, $R^2 = 0.82\text{--}0.92$) (B), ^1H NMR chemical shifts in chloroform versus water (slope = 1.0 , $R^2 = 0.98$) (C), and ^1H NMR chemical shifts in acetone versus water (slope = 0.8 , $R^2 = 0.89$) (D).

substituents that vary the donor–acceptor ΔpK_a over a wide range, and equilibrium hydrogen bond formation free energies (ΔG_f , defined in Figure 3A) measured for salicylates indicate stronger hydrogen bonds and a much steeper dependence on ΔpK_a in aprotic organic solvents than in water⁴² (see additional discussion in Text S3). In addition, as we describe below, multiple observations indicate that the hydrogen bond behavior of these intramolecular complexes is very similar to that of intermolecular complexes.

We acquired ^1H NMR spectra of a series of salicylates (aqueous ΔpK_a varied over 5 units) in chloroform ($\epsilon = 5$), acetone ($\epsilon = 21$), and water ($\epsilon = 80$), solvents of widely differing dielectric (ϵ) and hydrogen bonding ability. A far-downfield peak corresponding to the intramolecular hydrogen-bonded proton was readily detected in all spectra, including those obtained in water, where the downfield peak was mildly broadened due to slow exchange with bulk water (Figure 3A).

There were modest (<1 ppm) differences in the absolute chemical shift measured for each salicylate across the three solvents but no trend that distinguished the behavior between any of the solvents. Indeed, the ^1H NMR chemical shift measured for each salicylate’s hydrogen-bonded proton and its change across the series of salicylates were strikingly similar in all three solvent environments, with increases of 1.0 ± 0.1 ppm per unit decrease in ΔpK_a (Figure 3B). A plot of the observed ^1H NMR chemical shift in chloroform versus water is accurately

fit ($R^2 = 0.98$) by a linear function with a slope of 1.0 , further indicating a nearly identical dependence of hydrogen bond proton position on ΔpK_a in these two solvent environments despite their nearly 17-fold difference in dielectric constant and their disparate capacities to hydrogen bond with solutes (Figure 3C). Similar trends are seen for the observed ^1H NMR chemical shifts in acetone versus water ($R^2 = 0.89$) (Figure 3D), acetone versus chloroform ($R^2 = 0.89$) (Figure S1A), and water versus the previously reported²⁹ chemical shifts in 10% water/acetone ($R^2 = 0.92$) (Figure S1B). By plotting the NMR data in each solvent versus the NMR data in the other solvents, any uncertainty in the accuracy of the intrinsic ΔpK_a values for salicylates is eliminated from the analysis.

As noted above, ^1H NMR chemical shifts can be used to estimate hydrogen bond lengths^{34,43,44} and thus to quantify differences in hydrogen bond structure for the same salicylate or across the series of salicylates in discrete solvents (correlation functions given in Supporting Information and Materials and Methods). The hydrogen bond O–O distances estimated for 3,5-dinitrosalicylate in chloroform, acetone, and water were all within 0.01 \AA of one another and within 0.03 \AA of the O–O distance observed in a low-temperature neutron crystal structure of this compound (Table S2), providing additional evidence against substantial environmental effects on hydrogen bond length.

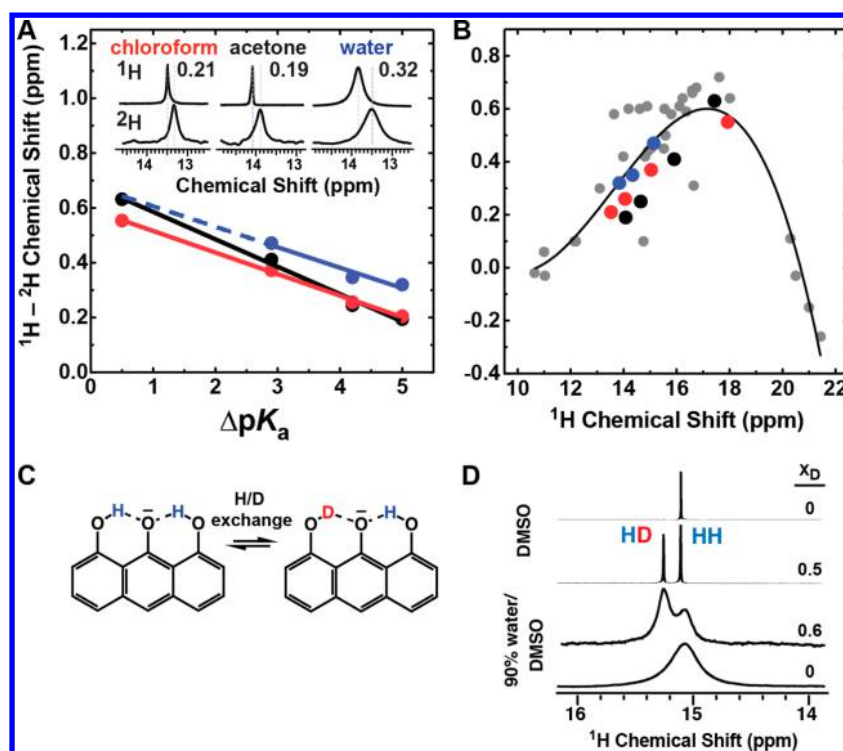


Figure 4. Deuterium isotope effects of hydrogen bond structure in water and organic solvents. (A) Dependence of the deuterium isotope shift (^1H - ^2H NMR chemical shift) on $\Delta\text{p}K_a$ in chloroform (red, $R^2 = 1.0$), acetone (black, $R^2 = 0.99$), and water (blue, $R^2 = 0.95$) for 5-methylsalicylate ($\Delta\text{p}K_a = 5.0$, spectra in inset), 4-methoxysalicylate ($\Delta\text{p}K_a = 4.2$), 5-formylsalicylate ($\Delta\text{p}K_a = 2.9$), and 3,5-dinitrosalicylate ($\Delta\text{p}K_a = 0.5$). (B) Plot of the deuterium isotope shift versus the ^1H NMR chemical shift for each salicylate in chloroform, acetone, and water (colors as in (A)) and for previously published O-H \cdots O $^-$ hydrogen-bonded complexes in aprotic organic solvents (gray).⁸ (C) The HH and HD isotopologues of 1,8,9-trihydroxyanthracene monoanion formed by partial deuterium exchange. (D) ^1H NMR spectra of the 1,8,9-trihydroxyanthracene monoanion in DMSO or 90% water/DMSO without or with partial deuterium exchange of labile hydrogen atoms. X_D = mole fraction of deuterium.

Across the series, the observed ^1H chemical shifts suggest that salicylate hydrogen bonds shorten by 0.02–0.03 Å (O \cdots O distance) and 0.04–0.05 Å (H \cdots O distance) per unit decrease in $\Delta\text{p}K_a$ in all three solvents.⁴⁹ These distance changes are very similar to the corresponding changes in O \cdots O (0.02 Å/ $\text{p}K_a$ unit) and H \cdots O (0.03 Å/ $\text{p}K_a$ unit) distances determined by neutron diffraction for hydrogen bonds in diverse small-molecule crystals (Figure 2A,B). Analysis of X-ray diffraction data in the Cambridge Structural Database for crystalline salicylates also indicate a 0.017 Å/ $\text{p}K_a$ unit change in O \cdots O distance that is nearly identical to that estimated by solution ^1H NMR for the salicylates and very similar to the 0.021 Å/ $\text{p}K_a$ unit change in O \cdots O distance observed by neutron diffraction for intermolecular hydrogen bonds (Figure S2). Thus, the physical properties of salicylate hydrogen bonds are not unique but are broadly similar to the observed behavior of the diverse inter- and intramolecular O-H \cdots O hydrogen bonds included in the crystallographic data sets (Figures S2 and S3, and additional discussion in Text S7). The 1.0 ± 0.1 ppm/ $\text{p}K_a$ unit change in chemical shift of the hydrogen-bonded proton across the series of salicylates in the three solvents is also identical, within error, to the 0.9 ± 0.2 ppm/ $\text{p}K_a$ unit chemical shift change reported for the intermolecular O-H \cdots O hydrogen bond between substituted phenols and trimethylamine-*N*-oxide in chloroform,³⁸ further supporting the conclusions that salicylate hydrogen bonds have similar properties to other hydrogen-bonded groups, including intermolecular complexes, and that hydrogen bond structure is not strongly influenced by solvent environment.

We also studied the effect of solvent on the hydrogen bond in 2-hydroxyphenylacetate, which, while still intramolecular, is less structurally constrained than the salicylates. Despite this additional flexibility, we observed nearly identical ^1H NMR chemical shifts for the hydrogen-bonded proton in chloroform (13.4 ppm) and 10% water/acetone (13.2 ppm) (Figure S9), providing additional evidence that supports our conclusion that solvent effects do not substantially alter the structures of intra- and intermolecular hydrogen bonds.

Probing Hydrogen Bond Potentials in Aprotic Solvents versus Water with ^2H Isotope Effects. To further test the conclusion that hydrogen bonds formed in water are not substantially lengthened relative to aprotic solvents and to evaluate possible differences in the potential energy surface of hydrogen bonds formed in different environments, we measured the deuterium (^2H) isotope effect on the NMR chemical shifts of the hydrogen-bonded protons. For hydrogen bonds with anharmonic potentials, substitution of the bridging proton for deuterium leads to a shortening of the O-D bond relative to the original O-H bond^{50,51} (most frequently observed in hydrogen bonds $< \sim 2.7$ Å) that can be detected by NMR as an upfield shift in the position of the ^2H peak relative to the ^1H peak.⁸ The magnitude of this ^1H - ^2H chemical shift has been observed to increase with decreasing hydrogen bond length, an effect ascribed to increased anharmonicity of the bond potential as the central barrier to proton transfer lowers with decreasing hydrogen bond length.⁵² Thus, measurement of the ^1H - ^2H chemical shift for a hydrogen bond provides an incisive readout of the general shape and anharmonicity of the potential energy surface.

We acquired ^2H NMR spectra for the same salicylates in chloroform, acetone, and water. The ^2H NMR peak in each case was readily detected for all compounds except for 3,5-dinitrosalicylate in water (Figure S4). The magnitudes of the ^1H – ^2H shifts observed for individual salicylates in distinct solvents were within 0.1 ppm of one another, and the change in the ^1H – ^2H shift as a function of ΔpK_a was nearly identical in the three environments (Figure 4A). In all cases the ^1H – ^2H shift increased similarly with increasing ^1H NMR chemical shift, as previously observed for diverse $\text{O}\cdots\text{H}\cdots\text{O}$ hydrogen bonds in nonaqueous solvents (Figure 4B) and as expected for progressively shorter hydrogen bonds whose individual anharmonicities and potential energy surfaces are very similar in both water and aprotic solvent environments.

Physical Coupling of Adjacent Hydrogen Bonds in Aprotic Solvents versus Water. Prior studies have observed that when two hydrogen bonds are donated to a common acceptor atom, substituting proton for deuterium in one of the hydrogen bonds results in a shortening of the neighboring hydrogen bond. This shortening can be detected as an increase in the ^1H NMR chemical shift of the hydrogen bond that retains its proton, and it indicates that the structures of the two hydrogen bonds are coupled.^{45,53}

To test whether water attenuates this coupling, as might occur if there were strong interactions with water molecules that changed the electronic properties of the hydrogen-bonded groups and altered the potential energy surface, we acquired ^1H NMR spectra of 1,8,9-trihydroxyanthracene monoanion (Figure S5) dissolved in DMSO or in 90% water/DMSO (this compound is insoluble in 100% water) without and with partial substitution of labile hydrogen atoms with deuterium (Figure 4C). Without deuterium exchange, we observed a single downfield ^1H NMR peak at 15.1 ppm in both solvents, corresponding to the two magnetically equivalent hydrogen-bonded protons of the symmetric $\text{O}\cdots\text{H}\cdots\text{O}\cdots\text{H}\cdots\text{O}$ isotopologue and reflecting nearly identical hydrogen bond structures in both solvent environments (Figure 4D). Upon partial deuteration, a second downfield peak was detected in both solvents, signaling formation of the $\text{O}\cdots\text{H}\cdots\text{O}\cdots\text{D}\cdots\text{O}$ isotopologue and indicating that these neighboring hydrogen bonds are coupled in both solvents. The observation that the downfield chemical shift of the $\text{O}\cdots\text{H}\cdots\text{O}\cdots\text{D}\cdots\text{O}$ isotopologue is the same (15.3 ppm), within error, in the aprotic and aqueous solvation environments, provides further evidence that hydrogen bonds have very similar structures and potential energy surfaces in both nonaqueous solvents and in water.

Theoretical Calculations of Hydrogen Bond Structure in Aprotic Solvents versus Water. Quantum mechanical (QM) calculations can, in principle, provide an independent and rigorous test of the effect of solvation on hydrogen bond structure, allowing discrete solvent properties to be separated and independently tested. However, computational complexities prevent modeling of both the hydrogen-bonded solutes and a full atomistic solvation environment at the highest levels of QM theory, and the development of accurate explicit solvation models remains an ongoing challenge.^{54,55}

To approach this question computationally, we first asked the most simple and computationally straightforward question of whether broadly varying the general solvent property of dielectric, in the absence of specific solvent–solute interactions, substantially alters hydrogen bond structure. We performed QM calculations on the water-hydroxide ion and formic acid-formate ion hydrogen bonds embedded in a polarizable

continuum⁵⁶ whose dielectric was varied between 5 and 80. This dielectric range mimics the dielectric difference between chloroform and water, two of the solvents tested experimentally and between which hydrogen bond ΔG_f values vary enormously. For both hydrogen bonds, *ab initio* calculations at multiple levels of theory and basis sets returned energy-minimized $\text{O}\cdots\text{O}$ and $\text{H}\cdots\text{O}$ distances near 2.5 and 1.5 Å, respectively, that increased by only 0.04 ± 0.01 Å as the continuum dielectric increased from 5 to 80 (Figures 5A and

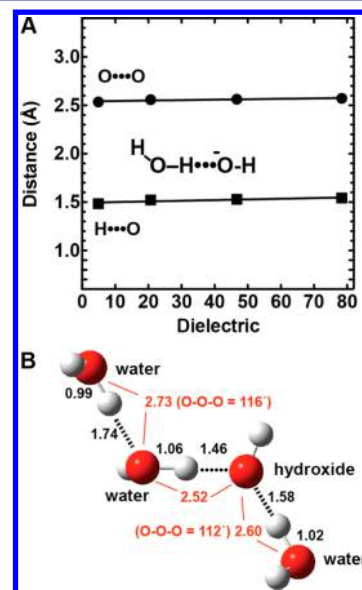


Figure 5. Theoretical calculations of the effect of solvent environment on hydrogen bond structure. Calculated structure of the water-hydroxide hydrogen bond in (A) a polarizable continuum of variable dielectric without explicit solvent or (B) a polarizable continuum with a dielectric value of 5 with two explicit water molecules. Distances are in angstroms (Å). Calculations were performed at the B3LYP level using the 6-311++G(d,p) basis set.

S6, Table S3, and additional discussion in Text S4). This small change is nearly identical to the 0.03 Å difference previously reported for the $\text{N}\cdots\text{H}\cdots\text{O}=\text{C}$ hydrogen bond ($\text{N}\cdots\text{O}$ and $\text{H}\cdots\text{O}$ distances) in the acetic acid-acetamide dimer at solvent dielectrics corresponding to water and chloroform.¹³ These results indicate that increasing solvent dielectric alone from the value of a low-polarity organic solvent such as chloroform to the value of water does not substantially perturb hydrogen bond structure.

To test whether intramolecular hydrogen bonds display a similar or different sensitivity to solvent dielectric compared to intermolecular hydrogen bonds, we performed analogous QM calculations for the intramolecular hydrogen bond in 5-methylsalicylate, one of the compounds studied experimentally herein (Table S3). Our calculations suggest that the $\text{O}\cdots\text{O}$ and $\text{H}\cdots\text{O}$ distances within this hydrogen bond increase by ≤ 0.02 Å as the dielectric increases from 5 to 80, supporting our conclusion that the structures of inter- and intramolecular hydrogen bonds display a similarly very low sensitivity to solvent dielectric.

Calculations using a continuum solvation model also afforded a straightforward means to test the effect of increasing solvent dielectric from 5 to 80 on the one-dimensional potential energy surface of the water-hydroxide ion hydrogen bond. These computations, summarized in Figure S7 and discussed in

more detail in Text S5, suggest that the shape of the potential energy well for O–H···O[−] hydrogen bonds is very similar at dielectric constants of 5–80, in agreement with our conclusion based on the ²H NMR studies above.

To address the computationally more complex question of whether specific hydrogen-bonding interactions between solutes and explicit solvating water molecules substantially lengthen hydrogen bonds compared to aprotic environments, we performed QM calculations on the water-hydroxide ion dimer at a dielectric of 5 that included two additional explicit hydrating water molecules (Figure 5B), and we compared the calculated distances to those obtained above in the absence of explicit hydration. These calculations gave a nearly identical O···O distance in the absence (2.535 Å) or presence (2.517 Å) of explicit hydrating water molecules (Figure 5B), consistent with the prior crystallographic observation that the presence or absence of two hydrating water molecules had nearly no effect on the length of the 4-nitrophenol:4-nitrophenolate hydrogen bond.³² Prior QM studies that involved more extensive solvation shells of explicit water molecules have also reported O···O distances of 2.5–2.6 Å for the water–hydroxide ion complex,^{57–59} suggesting that the very small length difference observed in our calculations plus or minus two hydrating water molecules is not substantially altered by inclusion of a larger network of solvating water molecules. Overall, these calculations suggest that the inductive effects on hydrogen bond structure from specific solvation by water molecules are small and on the order of ~ 0.02 Å, in contrast to prior suggestions in the literature that O–H···O hydrogen bonds are substantially lengthened in water relative to low polarity environments by as much as several tenths of an angstrom.^{12,16}

CONCLUSIONS AND IMPLICATIONS

Since Pauling's seminal description in *The Nature of the Chemical Bond*,²⁴ hydrogen bonds have been recognized as ubiquitous and critical interactions whose structural and energetic properties make dominant contributions to aqueous solvation and enormously influence the fundamental architectures and activities of all biological macromolecules. Hydrogen bonds formed within the complex interiors of folded biopolymers link together structural elements, tether bound ligands, and stabilize charge localization during enzymatic catalysis.

Although hydrogen bonds are present in bulk solution and in protein interiors, the nature of these two environments differs greatly. In aqueous solution, dissolved solutes are surrounded by extensive solvation shells of abundant water molecules, which can form hydrogen bonds with solutes and aggressively compete for hydrogen bond formation between solutes. Protein interiors, however, largely exclude water molecules and instead surround hydrogen-bonded groups with highly anisotropic solvation environments composed of structured arrays of charged, polar, and hydrophobic groups.

The effect of these solvation differences between the interior protein matrix and water on the structural and energetic properties of hydrogen bonds has been the subject of considerable debate and speculation in the literature and has remained unresolved.^{6,12,17,26,42,60} In this work, we have overcome longstanding technical limitations to determine the structural properties of hydrogen-bonded solutes in water. These direct and systematic measurements, in combination with prior studies of hydrogen bond formation free energies in water versus aprotic solvents, elucidate the fundamental

relationship between hydrogen bond length and stability in solution and have important implications for understanding hydrogen bond contributions to biomolecular function.

The Structural Properties of Hydrogen Bonds Show Little Sensitivity to Solvent Environment. We observed very similar structures for individual hydrogen bonds in widely differing solvent and crystalline environments (Figures S2B,C). Furthermore, the sensitivity of hydrogen bond length to changes in the proton affinity of the hydrogen bond donor and/or acceptor (ΔpK_a) was also nearly identical for diverse small molecules in water, aprotic solvents, and in crystals, with a 0.02–0.03 Å change in O···O distance per unit change in ΔpK_a (Figures 2A, 6B, and S2). This sensitivity is also nearly identical

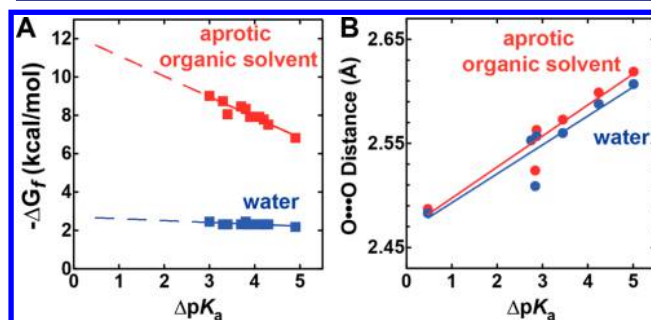


Figure 6. Hydrogen bond formation free energy but not hydrogen bond length is exquisitely sensitive to solvent. Comparison of the dependence of hydrogen bond formation energy (ΔG_f) (A) versus hydrogen bond O···O distance (B) on ΔpK_a for substituted salicylates in an aprotic organic solvent (red) versus water (blue). The ΔG_f values were previously published⁴² and were determined in DMSO and water. The O···O distances were determined from the ¹H NMR chemical shifts measured in chloroform and water as reported herein.

to that previously reported for a series of phenolates bound to ketosteroid isomerase^{61,62} (0.02 Å/ pK_a unit) or photoactive yellow protein⁵³ (0.03 Å/ pK_a unit), providing additional evidence for similar hydrogen bond structural properties across widely differing solvation environments.

Equilibrium distance is the most common read-out of hydrogen bond structure, but we have also probed the shape of the potential energy well for O–H···O[−] hydrogen bonds. High-level QM calculations (Figure S7) and indirect experimental measurements, including the ²H isotope effect on the NMR chemical shift of the hydrogen-bonded proton (Figure 4), suggest minimal changes in the hydrogen bond potential energy surface across solvents with widely varying dielectrics (5–80) and hydrogen-bonding ability (water versus aprotic).

Hydrogen bonds are shorter than the sum of the van der Waals radii of the interacting atoms, indicating a degree of orbital mixing and covalent character.^{24,63–65} Some degree of partial covalent character of hydrogen bonds could contribute to the minimal change in O–H···O[−] hydrogen bond structure across environments. Indeed, analogous covalent bond lengths in organic molecules vary little (e.g., 0.01–0.02 Å) in different solvent environments.^{66,67} The constancy of hydrogen bond lengths between protic and aprotic solvents may also arise because interaction energies of solvating water molecules with the oxygen atoms in an O–H···O[−] hydrogen bond are not sufficiently large, relative to the interaction energies within the O–H···O[−] complex, to perturb the electronic properties of the hydrogen-bonded groups and thereby reshape the potential energy well (see additional discussion in Text S6). Consistent

with this view, our QM calculations (Figure 5B) and prior theoretical^{57–59,68} and crystallographic³² studies suggest that the electronic perturbations due to the formation of additional hydrogen bonds to hydrating water molecules are small and result in only 0.01–0.02 Å changes in the length of a solute–solute hydrogen bond over the conditions investigated herein.⁶⁹ Indeed, even the presence of a second short (pK_a -matched) hydrogen bond only results in a minor <0.1 Å perturbation to a hydrogen bond formed to a common acceptor atom (Figure 5B),^{55,57,58} suggesting that even short hydrogen bonds do not greatly perturb the accessibility of the valence electron cloud for making an additional interaction.

Environment Rather than Hydrogen Bond Length Is the Primary Driving Force for Hydrogen Bond Stability.

Our findings clarify the physical basis for the widely differing hydrogen bond formation free energies for a given hydrogen bond pair in water versus aprotic environments. Large energetic differences (>8 kcal/mol) in the stability of individual hydrogen bonds in these discrete environments (Figures 1A and 6A) are not accompanied by large differences in hydrogen bond length (Figure 6B) or potential energy surface, disproving the central tenet of model II (Figure 1C) that hydrogen bond length and stability are directly coupled for a given complex. Hydrogen bond lengths for each compound studied changed only slightly (i.e., ~0.01–0.02 Å) in widely differing environments, indicating that hydrogen bond length is not the primary driving force for the more stable hydrogen bonding in low-dielectric and poorer solvating environments (see additional discussion in Text S6). Prior investigators have questioned the general connection between hydrogen bond structure and stability,^{2,12,68,70} and our work provides a direct and systematic test of this relationship.

By ruling out a significant contribution from model II, our results strongly favor model I,^{2,13,14} that the differences in hydrogen bond formation free energy for a given complex in protic versus aprotic solvents is dominated by the differential ability of these solvents to stabilize the dissociated donor and acceptor groups (Figure 1B, left side of equilibrium) (see additional discussion in Text S6). Solvation energies for the hydrogen-bonded groups (Figure 1B, right side of equilibrium) are also expected to differ in water versus aprotic environments. However, as is critical for the overall energetics of hydrogen bond formation, this difference is expected to be smaller than the corresponding difference for the isolated charge of the dissociated acceptor group. Our findings emphasize the need to understand the nature of the solvation environments in which hydrogen bonds form and to consider interactions with both sides of the equilibrium when analyzing hydrogen bond stability (ΔG_f) or any other equilibrium process.

The Origins of Changes in Hydrogen Bond Length and Formation Free Energies (ΔG_f) Across a Series of Hydrogen Bond Donors and Acceptors.

Although the length of a hydrogen bond for a particular complex is largely insensitive to solvent environment, hydrogen bond lengths across a series of compounds show a regular dependence on ΔpK_a , the proton affinity difference between the donor and acceptor groups (Figures 2 and 6B).^{37,68} This dependence on ΔpK_a holds whether the donor or acceptor is varied, and as noted above it displays a common dependence of 0.02–0.03 Å (O...O distance) per unit change in ΔpK_a ⁷¹ regardless of solution, crystalline, or protein environment (Figure S2).^{53,61,62}

Increased charge density of a hydrogen bond donor or acceptor group, which correlate strongly with pK_a ,^{72,73}

presumably results in larger electrostatic attractive forces and greater orbital mixing and covalent character between the hydrogen-bonded groups and thus shorter hydrogen bond distances with decreasing ΔpK_a . The formation free energy (ΔG_f) for hydrogen-bonded complexes also tends to vary linearly with ΔpK_a for a homologous series of compounds within a constant solvent environment.^{3,5,36,42} Overall, differences in hydrogen bond ΔG_f values across a series of compounds reflect changes in the hydrogen bond potential energy, from contributions classically ascribed to ionic and covalent factors as well as differential solvation effects for the free and hydrogen-bonded species for each complex in the series for each given solvent (see additional discussion in Text S6).

Short Hydrogen Bonds Inside Proteins Do Not Provide a Read-Out of Hydrogen Bond Stability or the Nature of the Local Electrostatic Environment.

Structural studies have identified short hydrogen bond distances (e.g., 2.4–2.6 Å) in the interior of numerous proteins, where they have been suggested to form due to unique properties of the solvent-sequestered protein matrix that differ from water and to make substantial energetic contributions to protein stability and function (e.g., catalysis).^{6,11,19} Our results demonstrate that formation of a short hydrogen bond within a protein or in other environments does not provide a read-out of the local solvation environment or hydrogen bond stability, as short lengths appear to be independent of solvent properties and are not tightly coupled to formation energy (Figure 6).

Several observations suggest the presence of slightly shorter hydrogen bonds within protein interiors than in other protein environments.^{17,74} Our results demonstrate that such differences are not expected from and do not reflect the local protein solvation environment and underscore the importance of exploring multiple potential origins. We speculate that packing and binding interactions within the anisotropic protein interior may constrain hydrogen bonds from relaxing to a preferred geometry in some instances, and such constraints might at times favor shorter^{17,74} or longer^{53,75} hydrogen bonds depending on the idiosyncrasies of the local structural environment. These complexities emphasize the need for direct, systematic tests of the structural and energetic contributions from hydrogen bonds in enzyme interiors,^{76,77} rather than inferring such contributions from distance observations alone.

Why Do Enzymes Exclude Water?

Recognition that hydrogen bond formation is generally weak in water compared to aprotic environments has led to proposals that hydrogen bonds are stronger (i.e., more stable) within the nonaqueous protein matrix because water molecules are largely excluded.^{11,17} Indeed, it is often stated that enzymes have evolved flexible surface loops or domains that close over active sites upon substrate binding in order to exclude water and thus to strengthen hydrogen bond formation.^{6,11,26,27,78–80}

Researchers have suggested that hydrogen bonds adopt shorter distances within enzymes upon better matching of proton affinities (pK_a values) between protein hydrogen bond donor groups and substrate acceptor groups in the reaction transition state due to water exclusion and that such shortening provides a mechanism to enhance hydrogen bond strength (i.e., potential energy) and thus stability.^{6,11,19} However, as noted above, our results provide direct evidence that the sensitivity of hydrogen bond distance to ΔpK_a is not strongly influenced by solvation environment or directly coupled to stability (Figure 6A,B), suggesting that modulation of hydrogen bond structure

via water exclusion is not a general mechanism for proteins to enhance hydrogen bond formation free energies.

Others have taken note of the general increase in hydrogen bond stability within nonaqueous environments and proposed that enzymes might exclude water in order to decrease the local polarity of active site as a mechanism to strengthen hydrogen bond formation and increase catalysis.^{17,26,27} To provide catalysis, however, enzymes must stabilize transition states relative to the stability of such species in aqueous solution. Enhanced stability of a hydrogen-bonded complex, which occurs for the case when both the dissociated groups and the complex are already in a nonaqueous environment (Figure 1B, bottom equilibrium), does not indicate that the hydrogen-bonded complex in a low polarity environment, in the absence of other active site features, is intrinsically more stable than that same complex in water and can thereby provide catalysis. Indeed, a destabilizing rather than stabilizing effect for a charged or polar hydrogen-bonded complex is expected upon lowering the environment polarity (Figure S8). In other words, all else being equal, the polar or charged complex would prefer to remain in the solvent of higher polarity or dielectric.

We suggest that enzymes have evolved domain closures and tightly packed active sites that largely exclude water molecules to optimally position and interact with bound substrates and thus maximize favorable binding interactions with active site groups whose electrostatic nature and geometric positioning are complementary to the shape and charge distribution of reaction transition state. It remains an ongoing experimental and computational challenge to understand the electrostatic nature of enzyme active sites, to fully decipher the physical consequences of excluding water, and to test the relative contributions to catalysis from positioning and charge stabilization and indeed to determine whether such factors are formally separable.^{60,75,81–85}

Implications for Computational Models. The strong correlation of hydrogen bond length with ΔpK_a suggests that expected values from such correlations might be used as benchmarks for computation and as simple checks of X-ray structural models. As there is evidence in certain situations for perturbations of hydrogen bond lengths by local structural features within proteins,^{53,75} a substantial mismatch to an expected value could indicate model error or interesting local interactions. In addition, as force fields often include empirical corrections, including terms to constrain hydrogen bond lengths could improve model accuracy. On an additional practical level, our observations suggest that molecular dynamics force fields will not require terms that mimic QM coupling between solvent molecules and hydrogen-bonded complexes to adjust the shape and depth of potential energy wells for hydrogen bonds in different environments. In addition, the near constancy of hydrogen bond distances across the range of solvation conditions and dielectric constants of 5–80 studied herein raises the possibility that benchmarking computational force fields to gas phase data may, in some instances, create unnecessary complications through the need for additional terms to adjust the hydrogen bond properties from those at very low dielectrics (i.e., 1–4) to those observed across a broad range of solvation conditions at higher solvent dielectrics.

MATERIALS AND METHODS

A full description of all experimental and computational methods is given in Supporting Information. Small-molecule neutron structures

were determined experimentally at the Intense Pulsed Neutron Source (Argonne National Laboratory) or retrieved from the Cambridge Structural Database and analyzed for hydrogen bond distances. ΔpK_a values were assigned based on experimental values or computational prediction. ¹H and ²H NMR spectra were acquired on 800 or 600 MHz Varian UNITYINOVA spectrometers equipped with a 5 mm, triple-resonance, gradient ¹H(¹³C/¹⁵N) probe, or a 10 mm broadband probe. NMR samples consisted of 25 mM substituted salicylic acid and triethylamine (TEA) in 100% water (containing 5% D₂O), acetone-*d*₆ (with 0.05% tetramethylsilane, TMS), or CDCl₃ (with 0.05% TMS). Spectra for samples dissolved in acetone-*d*₆, chloroform-*d*₆, and DMSO-*d*₆ were acquired using the s2pul pulse sequence, and chemical shifts were referenced internally to TMS (0 ppm). Spectra for aqueous samples were acquired using the 1331 binomial pulse sequence for water suppression, a 30 ppm spectral width (carrier frequency set on the water resonance), an excitation maximum of 14–17 ppm, and chemical shift referencing to the water resonance (5.0 ppm at 4 °C). Hydrogen bond distances were estimated from the measured ¹H NMR chemical shifts for the detected salicylate hydrogen-bonded protons using published correlation functions.^{34,44} QM calculations were performed at the HF, B3LYP, and MP2 levels using multiple basis sets.

ASSOCIATED CONTENT

Supporting Information

Additional discussion of hydrogen bond structure and energetics, additional analysis and comparison of structural properties of intra- and intermolecular hydrogen bonds, crystallographic coordinates and analysis of neutron structures, crystallographic data and refinement statistics, and QM calculated hydrogen bond distances. The Supporting Information is available free of charge on the ACS Publications website at DOI: 10.1021/ja512980h.

AUTHOR INFORMATION

Corresponding Author

*herschla@stanford.edu

Present Addresses

^VDepartment of Molecular Microbiology, Washington University, St. Louis, Missouri 63110

^{||}X-ray Science Division, Argonne National Laboratory, Argonne, Illinois 60439

Notes

The authors declare no competing financial interest.

ACKNOWLEDGMENTS

We thank J. Schwans, M. Miller, and P. Almond for assistance with NMR sample preparation, neutron crystallography, and X-ray crystallography, respectively. We thank J. Bowie, S. Benkovic, B. Cravatt, P. Kim, and C. Perrin for critical feedback on the manuscript. Funding was provided by NSF grant MCB-1121778 to D.H. P.A.S. is a recipient of a Burroughs Wellcome Fund Career Award at the Scientific Interface. Research at Argonne National Laboratory was supported by the U.S. Department of Energy, Office of Science, Office of Basic Energy Sciences, Materials Sciences and Engineering Division (Argonne Contract DE-AC02-06CH11357).

REFERENCES

- (1) We intentionally refrain from using the term “hydrogen bond strength”. This term, although widely adopted in the literature, lacks a precise or universally agreed definition but has typically referred to either a formation enthalpy (ΔH_f) or free energy (ΔG_f) change that reflects the energetic difference between the hydrogen-bonded complex and the dissociated donor and acceptor groups.
- (2) Guthrie, J. P. *Chem. Biol.* **1996**, *3*, 163–170.

- (3) Stahl, N.; Jencks, W. P. *J. Am. Chem. Soc.* **1986**, *108*, 4196–4205.
- (4) Shan, S. O.; Loh, S.; Herschlag, D. *Science* **1996**, *272*, 97–101.
- (5) Magonski, J.; Pawlak, Z.; Jasinski, T. *J. Chem. Soc. Faraday Trans.* **1993**, *89*, 119–122.
- (6) Cleland, W. W.; Frey, P. A.; Gerlt, J. A. *J. Biol. Chem.* **1998**, *273*, 25529–25532.
- (7) Cleland, W. W. *Arch. Biochem. Biophys.* **2000**, *382*, 1–5.
- (8) Hibbert, F.; Emsley, J. *Adv. Phys. Org. Chem.* **1990**, *26*, 255–379.
- (9) Zhao, Q. J.; Abeygunawardana, C.; Talalay, P.; Mildvan, A. S. *Proc. Natl. Acad. Sci. U.S.A.* **1996**, *93*, 8220–8224.
- (10) Perrin, C. L.; Nielson, J. B. *Annu. Rev. Phys. Chem.* **1997**, *48*, 511–544.
- (11) Frey, P. A.; Whitt, S. A.; Tobin, J. B. *Science* **1994**, *264*, 1927–1930.
- (12) Warshel, A.; Papazyan, A. *Proc. Natl. Acad. Sci. U.S.A.* **1996**, *93*, 13665–13670.
- (13) Pasalic, H.; Aquino, A. J.; Tunega, D.; Haberhauer, G.; Gerzabek, M. H.; Georg, H. C.; Moraes, T. F.; Coutinho, K.; Canuto, S.; Lischka, H. *J. Comput. Chem.* **2010**, *31*, 2046–2055.
- (14) Pasalic, H.; Tunega, D.; Aquino, A. J.; Haberhauer, G.; Gerzabek, M. H.; Lischka, H. *Phys. Chem. Chem. Phys.* **2012**, *14*, 4162–4170.
- (15) Kreevoy, M. M.; Liang, T. M. *J. Am. Chem. Soc.* **1980**, *102*, 3315–3322.
- (16) Gerlt, J. A.; Kreevoy, M. M.; Cleland, W. W.; Frey, P. A. *Chem. Biol.* **1997**, *4*, 259–267.
- (17) Gao, J.; Bosco, D. A.; Powers, E. T.; Kelly, J. W. *Nat. Struct. Mol. Biol.* **2009**, *16*, 684–690.
- (18) Bowie, J. U. *Curr. Opin. Struct. Biol.* **2011**, *21*, 42–49.
- (19) Cleland, W. W.; Kreevoy, M. M. *Science* **1994**, *264*, 1887–1890.
- (20) Lin, I. J.; Gebel, E. B.; Machonkin, T. E.; Westler, W. M.; Markley, J. L. *Proc. Natl. Acad. Sci. U.S.A.* **2005**, *102*, 14581–14586.
- (21) Feierberg, L.; Aqvist, J. *Biochemistry* **2002**, *41*, 15728–15735.
- (22) Perrin, C. L. *Science* **1994**, *266*, 1665–1668.
- (23) Mildvan, A. S.; Harris, T. K.; Abeygunawardana, C. *Methods Enzymol.* **1999**, *308*, 219–245.
- (24) Pauling, L. *The Nature of the Chemical Bond*; Cornell University Press: Ithaca, NY, 1960.
- (25) Jeffrey, G. A. *An Introduction to Hydrogen Bonding*; Oxford University Press: New York, 1997.
- (26) Richard, J. P.; Amyes, T. L.; Goryanova, B.; Zhai, X. *Curr. Opin. Chem. Biol.* **2014**, *21C*, 1–10.
- (27) Dewar, M. J.; Storch, D. M. *Proc. Natl. Acad. Sci. U.S.A.* **1985**, *82*, 2225–2229.
- (28) Lin, J.; Frey, P. A. *J. Am. Chem. Soc.* **2000**, *122*, 11258–11259.
- (29) Mock, W. L.; Morsch, L. A. *Tetrahedron* **2001**, *57*, 2957–2964.
- (30) Hess, R. A.; Reinhardt, L. A. *J. Am. Chem. Soc.* **1999**, *121*, 9867–9870.
- (31) Frey, P. A.; Cleland, W. W. *Bioorg. Chem.* **1998**, *26*, 175–192.
- (32) Marimanikkuppam, S. S.; Lee, I. S. H.; Binder, D. A.; Young, V. G.; Kreevoy, M. M. *Croat. Chem. Acta* **1996**, *69*, 1661–1674.
- (33) Venables, D. S.; Schmuttenmaer, C. A. *J. Chem. Phys.* **2000**, *113*, 11222–11236.
- (34) Jeffrey, G. A.; Yeon, Y. *Acta Crystallogr., Sect. B: Struct. Sci.* **1986**, *42*, 410–413.
- (35) Steiner, T.; Saenger, W. *Acta Crystallogr., Sect. B: Struct. Sci.* **1994**, *50*, 348–357.
- (36) Shan, S. O.; Herschlag, D. *Methods Enzymol.* **1999**, *308*, 246–276.
- (37) Gilli, P.; Pretto, L.; Bertolasi, V.; Gilli, G. *Acc. Chem. Res.* **2009**, *42*, 33–44.
- (38) Brycki, B.; Brzezinski, B.; Zundel, G.; Keil, T. *Magn. Reson. Chem.* **1992**, *30*, 507–510.
- (39) Zundel, G. *Adv. Chem. Phys.* **2000**, *111*, 1–217.
- (40) Roscioli, J. R.; McCunn, L. R.; Johnson, M. A. *Science* **2007**, *316*, 249–254.
- (41) Brycki, B.; Szafran, M. *J. Chem. Soc. Perkin. Trans. II* **1984**, 223–226.
- (42) Shan, S. O.; Herschlag, D. *Proc. Natl. Acad. Sci. U.S.A.* **1996**, *93*, 14474–14479.
- (43) McDermott, A.; Rydenour, C. F. In *Encyclopedia of NMR*; Grant, D. M., Harris, R. K., Eds.; John Wiley and Sons: Sussex, England, 1996; p 3820–3825.
- (44) Harris, T. K.; Mildvan, A. S. *Proteins* **1999**, *35*, 275–282.
- (45) Tolstoy, P. M.; Schah-Mohammed, P.; Smirnov, S. N.; Golubev, N. S.; Denisov, G. S.; Limbach, H. H. *J. Am. Chem. Soc.* **2004**, *126*, 5621–5634.
- (46) Harris, R. K.; Jackson, P.; Merwin, L. H.; Say, B. J.; Hagele, G. J. *Chem. Soc. Faraday Trans. I* **1988**, *84*, 3649–3672.
- (47) Rohling, C. M.; Allen, L. C.; Ditchfield, R. *J. Chem. Phys.* **1983**, *79*, 4958–4966.
- (48) Koeppe, B.; Guo, J.; Tolstoy, P. M.; Denisov, G. S.; Limbach, H. H. *J. Am. Chem. Soc.* **2013**, *135*, 7553–7566.
- (49) The change in O···O distance between 3,5-dinitrosalicylate and 5-nitrosalicylate estimated by solution ^1H NMR (0.055 Å) is very similar to the distance difference (0.046 Å) observed between the neutron structure of 3,5-dinitrosalicylate (O···O distance = 2.516 Å, Table S1) and an unpublished X-ray structure of 5-nitrosalicylate (O···O distance 2.562 Å), providing additional support for our use of NMR to estimate changes in salicylate hydrogen bond lengths.
- (50) Ichikawa, M. *Acta Crystallogr., Sect. B: Struct. Sci.* **1978**, *34*, 2074–2080.
- (51) Ichikawa, M. *J. Mol. Struct.* **2000**, *552*, 63–70.
- (52) Altman, L. J.; Laungani, D.; Gunnarsson, G.; Wennerstrom, H.; Forsen, S. *J. Am. Chem. Soc.* **1978**, *100*, 8264–8266.
- (53) Sigala, P. A.; Tsuchida, M. A.; Herschlag, D. *Proc. Natl. Acad. Sci. U.S.A.* **2009**, *106*, 9232–9237.
- (54) Guillot, B. *J. Mol. Liq.* **2002**, *101*, 219–260.
- (55) Jorgensen, W. L.; Tirado-Rives, J. *Proc. Natl. Acad. Sci. U.S.A.* **2005**, *102*, 6665–6670.
- (56) Tomasi, J.; Mennucci, B.; Cammi, R. *Chem. Rev.* **2005**, *105*, 2999–3093.
- (57) Pliego, J. R.; Riveros, J. M. *J. Chem. Phys.* **2000**, *112*, 4045–4052.
- (58) Lee, H. M.; Tarkeshwar, P.; Kim, K. S. *J. Chem. Phys.* **2004**, *121*, 4657–4664.
- (59) Chaudhuri, C.; Wang, Y. S.; Jiang, J. C.; Lee, Y. T.; Chang, H. C.; Niedner-Schatteburg, G. *Mol. Phys.* **2001**, *99*, 1161–1173.
- (60) Warshel, A.; Aqvist, J.; Creighton, S. *Proc. Natl. Acad. Sci. U.S.A.* **1989**, *86*, 5820–5824.
- (61) Kraut, D. A.; Sigala, P. A.; Pybus, B.; Liu, C. W.; Ringe, D.; Petsko, G. A.; Herschlag, D. *PLoS Biol.* **2006**, *4*, e99.
- (62) Hanoian, P.; Sigala, P. A.; Herschlag, D.; Hammes-Schiffer, S. *Biochemistry* **2010**, *49*, 10339–10348.
- (63) Isaacs, E. D.; Shukla, A.; Platzman, P. M.; Hamann, D. R.; Barbiellini, B.; Tulk, C. A. *Phys. Rev. Lett.* **1999**, *83*, 4445–4445.
- (64) Stevens, E. D.; Lehmann, M. S.; Coppens, P. *J. Am. Chem. Soc.* **1977**, *99*, 2829–2831.
- (65) Grzesiek, S.; Cordier, F.; Dingley, A. J. *Methods Enzymol.* **2001**, *338*, 111–133.
- (66) Torii, H.; Tatsumi, T.; Tasumi, M. *J. Raman Spectrosc.* **1998**, *29*, 537–546.
- (67) Andzelm, J.; Kolmel, C.; Klamt, A. *J. Chem. Phys.* **1995**, *103*, 9312–9320.
- (68) Chen, J. G.; McAllister, M. A.; Lee, J. K.; Houk, K. N. *J. Org. Chem.* **1998**, *63*, 4611–4619.
- (69) Our computations and prior results suggest that larger differences in hydrogen bond O···O or H···O distance on the scale of 0.03 – 0.1 Å or larger may occur when comparing distances calculated at dielectric values ≥ 5 to calculations at dielectric values of 1.0 (vacuum) or 1.4 (argon gas) (Table S3). As the physical transition from a vacuum to solvent (including polarizable continuum models) is complex, additional theoretical work will be needed to understand structural changes in this very low dielectric region.
- (70) Perrin, C. L. *Acc. Chem. Res.* **2011**, *43*, 1550–1557.
- (71) We emphasize that we have used a common pK_a scale for all compounds in water, regardless of the specific solvent environment

studied, and that the value of ΔpK_a itself is not the cause of the varying hydrogen bond length but rather shares a common sensitivity with hydrogen bond length to other molecular properties, especially atomic charge density.

(72) Gross, K. C.; Seybold, P. G. *Int. J. Quantum Chem.* **2001**, *85*, 569–579.

(73) Gross, K. C.; Seybold, P. G.; Hadad, C. M. *Int. J. Quantum Chem.* **2002**, *90*, 445–458.

(74) Joh, N. H.; Min, A.; Faham, S.; Whitelegge, J. P.; Yang, D.; Woods, V. L.; Bowie, J. U. *Nature* **2008**, *453*, 1266–U1273.

(75) Sigala, P. A.; Kraut, D. A.; Caaveiro, J. M.; Pybus, B.; Ruben, E. A.; Ringe, D.; Petsko, G. A.; Herschlag, D. *J. Am. Chem. Soc.* **2008**, *130*, 13696–13708.

(76) Kraut, D. A.; Sigala, P. A.; Fenn, T. D.; Herschlag, D. *Proc. Natl. Acad. Sci. U.S.A.* **2010**, *107*, 1960–1965.

(77) Schwans, J. P.; Sunden, F.; Gonzalez, A.; Tsai, Y. S.; Herschlag, D. *J. Am. Chem. Soc.* **2011**, *133*, 20052–20055.

(78) Malabanan, M. M.; Amyes, T. L.; Richard, J. P. *Curr. Opin. Struct. Biol.* **2010**, *20*, 702–710.

(79) Perutz, M. *Proc. R. Soc. London, Ser. B* **1967**, *167*, 448.

(80) Wierenga, R. K.; Kapetaniou, E. G.; Venkatesan, R. *Cell. Mol. Life Sci.* **2010**, *67*, 3961–3982.

(81) Fafarman, A. T.; Sigala, P. A.; Schwans, J. P.; Fenn, T. D.; Herschlag, D.; Boxer, S. G. *Proc. Natl. Acad. Sci. U.S.A.* **2012**, *109*, E299–308.

(82) Natarajan, A.; Schwans, J. P.; Herschlag, D. *J. Am. Chem. Soc.* **2014**, *136*, 7643–7654.

(83) Sigala, P. A.; Fafarman, A. T.; Bogard, P. E.; Boxer, S. G.; Herschlag, D. *J. Am. Chem. Soc.* **2007**, *129*, 12104–12105.

(84) Jha, S. K.; Ji, M.; Gaffney, K. J.; Boxer, S. G. *Proc. Natl. Acad. Sci. U.S.A.* **2011**, *108*, 16612–16617.

(85) Chimentì, M. S.; Castaneda, C. A.; Majumdar, A.; Garcia-Moreno, E. B. *J. Mol. Biol.* **2011**, *405*, 361–377.